

Assessment of Langatate Material Constants and Temperature Coefficients Using SAW Delay Line Measurements

Blake T. Sturtevant^{1,3} and Mauricio Pereira da Cunha^{2,3}

Department of Physics¹

Department of Electrical & Computer Engineering²

Laboratory for Surface Science & Technology³

University of Maine, Orono, Maine USA

mdacunha@eece.maine.edu

Abstract— This paper reports on the assessment of LGT acoustic material constants and temperature coefficients by surface acoustic wave (SAW) delay line measurements up to 130 °C. Based upon a full set of material constants recently reported by the authors, seven orientations in the LGT plane with Euler angles (90°, 23°, Ψ°) were identified for testing. Each of the seven selected orientations exhibited predicted coupling coefficients (K^2) between 0.2% and 0.75% and also showed a large range of predicted temperature coefficient of delay (TCD) values around room temperature. Additionally, methods for estimating the uncertainty in predicted SAW propagation properties were developed and applied to SAW phase velocity and temperature coefficient of delay calculations. Starting from a purchased LGT boule, the SAW wafers used in this work were aligned, cut, ground, and polished at University of Maine facilities, followed by device fabrication and testing. Using repeated measurements of two devices on separate wafers for each of the seven orientations, the room temperature SAW phase velocities were extracted with a precision of 0.1% and found to be in agreement with the predicted values. The normalized frequency change and the temperature coefficient of delay for all seven orientations agreed with predictions within the uncertainty of the measurement and the predictions over the entire 120 °C temperature range measured. Two orientations, with Euler angles (90°, 23°, 123°) and (90°, 23°, 119°), were found to have high predicted coupling for LGT ($K^2 > 0.5\%$) and were shown experimentally to exhibit temperature compensation in the vicinity of room temperature, with turnover temperatures at 50 and 60 °C, respectively.

I. INTRODUCTION

Langatate (LGT, $\text{La}_3\text{Ga}_{5.5}\text{Ta}_{0.5}\text{O}_{14}$) has been considered for the past twenty years as a promising piezoelectric material for applications in frequency control, wireless communications, and sensors [1-9]. LGT belongs to the crystal point group 32, the same as quartz, berlinite, and gallium phosphate, and shows potential to simultaneously exhibit increased electromechanical coupling compared to quartz and temperature compensation orientations [10, 11]. Attractive

properties of LGT include piezoelectric constants e_{11} and e_{14} that are 2-4 times higher than those of quartz, the absence of phase changes and the retention of piezoelectricity up to its melting point of 1470 °C, high density (6147 kg/m³), and reported surface and bulk acoustic wave (SAW and BAW) orientations with temperature compensation [2, 9, 11, 12].

LGT orientations exhibiting temperature compensation around room temperature have previously been predicted based on published acoustic material constants [2, 12], but experimentally observed orientations of temperature compensation have occurred at temperatures up to 100 °C away from room temperature [2]. Further, the literature on LGT acoustic wave material properties contains many discrepancies, some of them large, in particular for the values of the elastic and piezoelectric constants and their temperature coefficients as discussed in detail in [9]. It is not presently clear to what extent these discrepancies in the reported material constants and temperature coefficients arose from different or imprecise measurement techniques, variations in the crystal composition and structure in materials provided by different growers, or yet some other reason to be determined [9, 13, 14]. In an attempt to re-examine the LGT material constants and temperature coefficient, a carefully determined set of elastic and piezoelectric constants and temperature coefficients has recently been extracted by pulse echo overlap and combined resonance techniques [9]. In that work, use was made of expansion coefficient measurements [15] and dielectric constant and respective temperature coefficient measurements [16] performed under the same project.

The present work focuses on the assessment of these recently reported material constants and temperature coefficients by using SAW delay line devices fabricated using LGT boules originating from the same crystal supplier reported in [9, 15, 16]. Room temperature phase velocities, v_p , and temperature coefficient of delay (TCD) are extracted through S_{21} delay line frequency response measurements. The experimentally obtained v_p and TCD are then compared with those numerically predicted using the constants in [9]. Normalized frequency variations and TCD as a function of temperature are also reported in this work and compared with predictions to verify the temperature coefficients given in [9]. A method for estimating the uncertainties in the predicted v_p

Financial support for this work was provided in part by the Army Research Office ARO Grant #DAAD19-03-1-0117, by the Petroleum Research Fund Grant ACS PRF# 42747-AC10, by the National Science Foundation grants # ECS 0134335 and # DGE-0504494, and the Air Force Office AFO Grant # FA9550-07-1-0519.

and TCD is developed based upon the uncertainties in the material properties, in order to assess the agreement between the measured and predicted v_p and TCD.

Section II presents experimental details including plane selection, device fabrication, SAW phase velocity measurements, and experimental uncertainties. Section III describes how the uncertainties in the predicted SAW parameters of v_p and TCD can be estimated provided that the uncertainties in the material constants are known. Section IV discusses the experimental results and the consistency between measurement and prediction. Finally, Section V concludes the paper.

II. EXPERIMENTAL PROCEDURE

A. SAW Plane Selection

Using a full set of acoustic material constants (elastic, piezoelectric, and dielectric constants as well as density) and their respective temperature coefficients determined from a single LGT boule [9, 15, 16], a numerical search procedure was conducted for planes suitable for SAW evaluation. The two criteria used for selecting a plane for SAW fabrication were: (i) that the plane had sufficiently high electromechanical coupling (K^2) to allow the probing of all SAW propagation directions of interest within the plane; (ii) that the plane exhibited a wide range of TCD which is useful for verifying the temperature coefficients of the elastic and piezoelectric constants; (iii) if possible, use a single rotated cut or double rotated cuts with initial surface normals lying in the Y-Z, X-Z, and X-Y planes for maximum use of the material and easier alignment. For the search of the crystal cut, two Euler angles were varied at a time in each of three separate searches. The three searches investigated the spaces defined by Euler angles: $(0^\circ, \Theta^\circ, \Psi^\circ)$, $(90^\circ, \Theta^\circ, \Psi^\circ)$, and $(\Phi^\circ, 90^\circ, \Psi^\circ)$, corresponding to wafers with surface normals lying in the Y-Z, X-Z, and X-Y planes, respectively.

B. Device Fabrication

The wafers' alignment, cutting, grinding, polishing, and the SAW device design, fabrication, and testing were performed at the Microwave Acoustics Material Lab, Laboratory for Surface Science and Technology facilities at the University of Maine (UMaine). Wafers for SAW fabrication were cut using an inner diameter saw (Meyer-Berger, Steffisberg, Switzerland) from a single crystal LGT boule (Fomos Materials, Moscow, Russia) which was purchased at the same time as the material used for the determination of material constants reported in [9, 15, 16]. Wafers were aligned to the selected orientation to better than six arcminutes using a PANalytical X'Pert Pro Materials Research Diffractometer (PANalytical, Inc., Natick, MA) using techniques described in [17, 18]. The wafers were mechanically ground using Al_2O_3 abrasives (Micro Abrasives Corporation, Westfield, MA) of decreasing grit size down to $1\ \mu\text{m}$ and then polished to an optical finish using colloidal silica (Universal Photonics, Hicksville, NY). Two identical sets of seven SAW delay lines, shown in Fig. 1, were fabricated on the polished substrates using $1500\ \text{\AA}$ of aluminum on top of a $150\ \text{\AA}$ chromium adhesion layer. Split

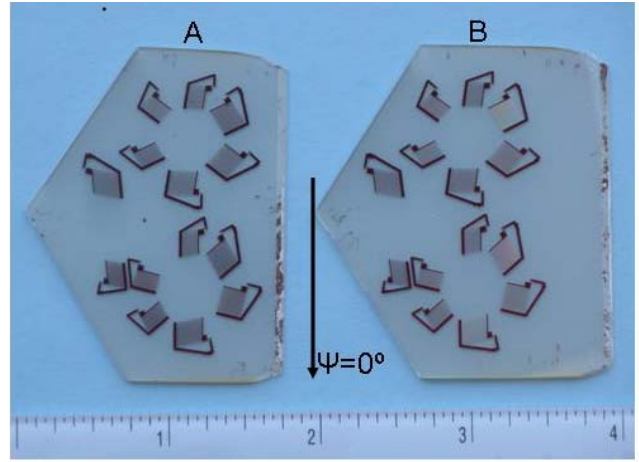


Figure 1. The two wafers fabricated, each with seven SAW delay line devices. The arrow denotes the $(90^\circ, 23^\circ, 0^\circ)$ propagation direction and the ruler scale is inches.

finger electrodes were used to reduce the triple transit response of the devices. Each finger had a width of $4\ \mu\text{m}$, yielding a SAW wavelength of $\lambda=32\ \mu\text{m}$ at the IDT. The non-zero power flow angle (PFA) was accounted for in the design and fabrication of delay lines along the seven orientations selected in this work. The delay lines were designed to have one transducer with an acoustic aperture of 80λ and the second transducer with an aperture of 130λ to ensure that the SAWs were measurable despite variations in the PFA as a function of temperature. All transducers had an active length of $125\ \lambda$, and the IDT center-to-center delay path was between 455 and $475\ \lambda$ for the devices. The electrically open, mechanically unloaded delay path was chosen to be as large as possible for the prepared wafers (~ 3 times the length of the transducer) to minimize the influence of the electrodes on the propagation path.

C. SAW S_{21} Frequency Measurements

The S_{21} center frequency response of the devices was measured using an RF probe station (Cascade Microtech, Inc., Beaverton, OR) and an Agilent 8753 ES network analyzer (Agilent Technologies, Santa Clara, CA). Time gating was used to remove electromagnetic feed-through, residual SAW triple transit, and other spurious acoustic reflections. The gated S_{21} response was recorded and the maximum of $|S_{21}|$ was recorded as the center frequency for each measurement. The temperature of the devices was controlled using a Temptronic thermal chuck with $0.1\ ^\circ\text{C}$ precision. Due to the thermal gradient between the chuck and the top surface of the LGT substrate, the temperature measured by the Temptronic controller starts to diverge from the actual temperature of the SAW device once the thermal chuck departs from room temperature, with the discrepancy increasing with temperature. To more accurately determine the SAW operating temperature, a secondary RTD was mounted on top of an LGT wafer of the same thickness as the device substrate and was used to record the temperature at the surface of the LGT substrates during all measurements. A $5\ ^\circ\text{C}$ difference between the operating temperature of the SAW and the

temperature measured by the Temptronic controller was registered at 130 °C.

At room temperature (25.0 °C), the frequency response of each of the fourteen devices (seven devices on each of two wafers, labeled 'A' and 'B' in Fig. 1) was measured five times to determine the precision of the frequency measurement for each device. The mean and the standard error of the frequency measurements were taken as the measured frequency, f , and the uncertainty in the measured frequency, δ_f , of each device, respectively. The SAW phase velocity, v_p , with associated uncertainty, δ_{v_p} , were then calculated through the wave relationship by:

$$v_p = \lambda f, \quad (1a)$$

$$\delta_{v_p} = \sqrt{\lambda^2 (\delta f)^2}, \quad (1b)$$

since the uncertainty in the photolithographically defined wavelength, λ , was considered negligible.

To determine the thermal properties of the SAWs, frequency measurements were made using the seven devices on wafer 'A' at temperatures between 10 and 130 °C. The RF probe tips were lifted off of the device before changing the temperature to avoid destruction of the device and probe tips caused by the thermal expansion of the LGT. The required repeated lifting off and replacement of the probe tips during the temperature runs ends up scratching away the aluminum electrodes and for this reason it was decided to perform temperature measurements on only one of the two fabricated wafers. Measurements were made at 10 °C intervals for five of the seven devices, and at 5 °C intervals for the remaining two devices. The reason for making measurements with higher temperature resolution for two of the devices was to accurately determine the turnover temperature since these orientations exhibit temperature compensation near room temperature. The normalized frequency variation for each device was calculated by:

$$\Delta f(T) / f_0 = \frac{f(T) - f(25^\circ\text{C})}{f(25^\circ\text{C})}. \quad (2)$$

Similarly, TCD was calculated by:

$$TCD(T) = \frac{-1}{f(T)} \frac{f(T + \varepsilon) - f(T - \varepsilon)}{2\varepsilon} \quad (3)$$

where the minus sign in (3) results from the relation of TCD and the temperature coefficient of frequency, $TCF = -TCD$, and ε is a small change temperature change, either 5 or 10 °C, depending on the device being considered. The precision in the measurement of temperature was high enough that the error in temperature measurements contributed a negligible amount to the uncertainty in the measured $\Delta f/f_0$ and TCD , so the uncertainty in these quantities was calculated by propagating the uncertainty in the measured frequencies.

III. CALCULATED SAW PARAMETER UNCERTAINTY

The methods governing the calculation of LGT SAW phase velocity for electrically open and shorted surfaces, needed for the calculation of SAW parameters including: v_p ,

TCD , K^2 , PFA, acoustic diffraction, and wave polarization are described elsewhere [2, 12, 19] and will not be further discussed here. This section focuses on the estimation of uncertainty in the calculated v_p and TCD , based upon the uncertainty in the acoustic material constants used in the calculations and the sensitivity of the SAW along a specific orientation to the different material constants.

As a point group 32 crystal, LGT has six independent elastic constants, C_k , where the index k represents here the six elastic constants of LGT. If one considers only the influence of the elastic constants on the phase velocity error, this error becomes:

$$\delta_{v_p}^C = \sqrt{\sum_k \left(\frac{\partial v_p}{\partial C_k} \right)^2 (\delta C_k)^2}. \quad (4)$$

The superscript 'C', in $\delta_{v_p}^C$, is used to denote uncertainty in a calculated, as opposed to a measured, quantity. The exclusion of the piezoelectric constants in LGT SAW calculations influences the SAW phase velocity by less than 2% for all propagation directions in the (90°, 23°, Ψ) plane. Because the piezoelectric and dielectric constants have such a reduced influence on the LGT SAW propagation properties, the errors in the calculated v_p and TCD were assumed to depend solely on the errors in the elastic constants.

Unlike the case with bulk acoustic waves where analytical solutions for $\partial v_p / \partial C_{ij}$ exist, this quantity generally must be computed numerically for SAWs. These quantities were determined for each of the seven measured SAWs by calculating the SAW phase velocity using a slightly higher value for the six elastic constants. For example, to determine the sensitivity of a SAW to elastic constant C_{11} , this sensitivity was calculated by:

$$\frac{\partial v_p}{\partial C_{11}} = \frac{v_p(C_{11} * 1.01) - v_p(C_{11})}{0.01 * C_{11}} \quad (5)$$

The partial derivatives were carried out by varying only one constant at a time, holding all others constant, for each of the seven SAW propagation directions. The sensitivity of each of the modes to the six elastic constants is displayed in Table I.

The predicted TCD of the SAWs was calculated using the expression [20]:

$$TCD = \frac{1}{l} \frac{dl}{dT} - \frac{1}{v_p} \frac{dv_p}{dT} = TCE - TCv \quad (6)$$

Where l is the SAW wavelength and TCE and TCv are the temperature coefficients of expansion and velocity, respectively. From this expression, the uncertainty in the calculated TCD , δ_{TCD}^C , can be written:

$$\delta_{TCD}^C = \sqrt{(\delta_{TCE})^2 + \left(\frac{1}{v_p^2} \frac{dv_p}{dT} \right) (\delta_{v_p})^2 + \left(\frac{1}{v_p} \right)^2 \left(\delta \frac{dv_p}{dT} \right)^2}, \quad (7)$$

where the uncertainty in the temperature derivative of phase velocity is calculated using the uncertainty in the temperature

TABLE I. SENSITIVITY OF SAWS TO THE SIX ELASTIC CONSTANTS

	$\partial v_p / \partial C_{ij} \text{ (m s}^{-1} \text{ Pa}^{-1}) * 10^{-10}$						
	$\Psi=0^\circ$	$\Psi=13^\circ$	$\Psi=48^\circ$	$\Psi=77^\circ$	$\Psi=119^\circ$	$\Psi=123^\circ$	$\Psi=170^\circ$
C_{11}	4	4	4	3	10	6	1
C_{13}	-6	-4	-7	-6	-12	-8	-2
C_{14}	-190	-260	-260	-280	-51	4	-190
C_{33}	2	2	4	3	5	3	1
C_{44}	55	101	75	80	83	28	46
C_{66}	263	223	248	257	179	236	287

coefficients of the elastic constants, since the partial derivative of the phase velocity with respect to the elastic constants is a property of the crystal geometry:

$$\delta \frac{dv_p}{dT} = \sqrt{\sum_k \left(\frac{\partial v_p}{\partial C_k} \right)^2 \left(\delta \frac{dC_k}{dT} \right)^2}. \quad (8)$$

IV. RESULTS AND DISCUSSION

A. SAW Plane Selection

The plane selected for device fabrication has Euler angles $[\Phi, \Theta, \Psi] = [90^\circ, 23^\circ, \Psi]$, with a surface normal vector making angles of 23° and 67° with the +Z and +X axes, respectively, and a $\Psi=0^\circ$ propagation direction along the +Y crystalline axis. Fig. 2 shows the calculated SAW coupling and TCD for this plane. The plane has calculated SAW coupling higher than that of ST-X quartz ($K^2=0.11\%$) throughout most of the plane and exhibits K^2 as high as 0.75% in a region where TCD is expected to be near zero around room temperature ($110^\circ \leq \Psi \leq 130^\circ$). The seven orientations for which devices were fabricated were chosen based on their predicted coupling ($K^2 > 0.2\%$) and their large range of predicted TCDs ($-64 \leq \text{TCD} \leq 4 \text{ ppm}/^\circ\text{C}$), allowing for an assessment of the elastic temperature coefficients. The seven orientations measured have azimuthal angles of $\Psi = 0^\circ, 13^\circ, 48^\circ, 77^\circ, 119^\circ, 123^\circ$, and 170° (Fig. 2).

B. Room Temperature SAW Phase Velocities

For each of the fourteen devices, the average frequency of repeated measurements was used to calculate the phase

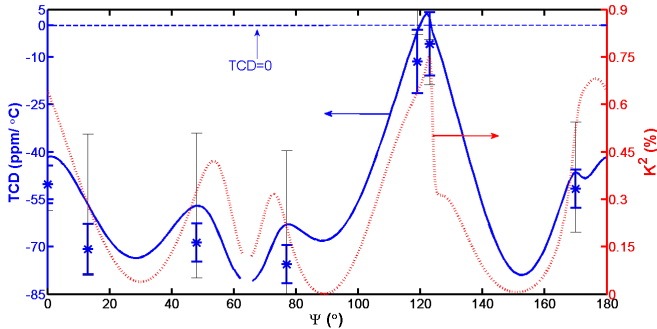


Figure 2. TCD (solid, left axis) and K^2 (dashed, right axis) for the plane measured (Euler angles $90^\circ, 23^\circ, \Psi$). Measured TCDs are indicated with asterisks. The thin error bars correspond to the predicted TCDs.

velocity of that device, and the standard error was used as the uncertainty. Although five measurements were made on each device, one set of measurements on wafer ‘A’ were discarded as outliers because the values were more than two standard deviations away from the mean of the five measurements. The phase velocities of each duplicate pair of devices with the same propagation direction were compared and agreed within the uncertainty of the measurements. The phase velocity for each propagation direction was then computed as the average of the velocities for each pair of devices with the same orientation. The phase velocities determined for each of the seven SAW propagation directions are displayed in Table II where all of them have an uncertainty of $\pm 2 \text{ m/s}$ or $\sim 0.1\%$. Table II also presents the predicted phase velocities, each of which has an uncertainty of $\pm 10 \text{ m/s}$ calculated using (4) and the reported uncertainties in [9]. Reference [9], which reported on LGT elastic constants determined by BAW measurements, reports two different sets of uncertainties for the elastic constants, one of which was determined analytically and another which was estimated through an optimization routine. The uncertainties determined by the optimization routine were larger and are the uncertainties used in the calculations of this work. It should be noted that if the analytically determined elastic constants are used instead, the uncertainty in the predicted SAW v_p is reduced to $\sim 3 \text{ m/s}$ for each SAW, which is still in agreement with the measured v_p .

C. SAW Temperature Behavior

The TCD for each of the seven orientations were determined from measurements between 10 and 130°C using (3). The predicted room temperature TCDs are shown in Fig. 2 and in Table II and are based upon the constants published in [9]. Table II also presents the uncertainties for the predicted TCDs along the selected orientations calculated using (7). Uncertainties in the temperature derivatives of the elastic constants are critical for the estimation of uncertainty in temperature related SAW parameters. The dC_{ij}/dT from [9] and the associated $\delta \frac{dC_{ij}}{dT}$ which were used in this work are shown in Table III. For simplicity, the symbol δ_{ij} is used in Table III and in the text to denote $\delta \frac{dC_{ij}}{dT}$. It can be noted from

Table II that the uncertainty in the measured TCD for the $\Psi=119^\circ$ and $\Psi=123^\circ$ SAWs is slightly larger than the uncertainty for the other five orientations, owing to the fact

TABLE II. MEASURED AND PREDICTED ROOM TEMPERATURE (25°C) SAW PROPERTIES

$\Psi(^\circ)$	Measured			Predicted		
	v_p^a (m/s)	TCD (ppm/ $^\circ\text{C}$)	δ_{TCD} (ppm/ $^\circ\text{C}$)	v_p^b (m/s)	TCD (ppm/ $^\circ\text{C}$)	δ_{TCD} (ppm/ $^\circ\text{C}$)
0	2445	-50	6	2449	-42	17
13	2335	-71	8	2338	-57	22
48	2311	-69	6	2310	-57	23
77	2327	-76	6	2326	-64	24
119	2730	-12	10	2720	4	7
123	2752	-6	10	2756	-12	7
170	2430	-52	6	2430	-48	17

a. measured v_p , all $\pm 2 \text{ m/s}$

b. predicted v_p , all $\pm 10 \text{ m/s}$

TABLE III. TEMPERATURE DERIVATIVE OF ELASTIC CONSTANTS

C_{ij}	dC_{ij}/dT (MPa/°C)	δ_{ij} (MPa/°C)
C_{11}	-13.5	0.1
C_{13}	8.4	2
C_{14}	-4.9	2
C_{33}	-22.3	0.1
C_{44}	-0.05	0.3
C_{66}	0.6	0.8

that the measurements for these two orientations were made at smaller temperature intervals, which is necessary to accurately determine the turnover temperature.

The predicted uncertainty in the TCD is dominated by the third term under the square root sign in (7). The uncertainty in the predicted TCDs of the seven SAWs studied here is almost entirely attributable to δ_{14} , which reflects: (i) the large v_p sensitivity to C_{14} for most of the SAW orientations listed in Table I and (ii) the considerable value of δ_{14} which can be seen in Table III. Though the sensitivity of the v_p to C_{66} is of the same order as that for C_{14} , δ_{66} is only half as large as δ_{14} , leading to a reduced influence of C_{66} to δ_{TCD}^C . Because of the

reduced sensitivity to C_{14} of the $\Psi=119^\circ$ and $\Psi=123^\circ$ SAWs, δ_{TCD}^C for these waves is reduced to $\sim 1/3$ of the uncertainty for the other five orientations.

The measured TCD for all seven orientations was in agreement with predicted values, within their associated uncertainties, over the entire temperature range measured. As an example of the temperature behavior of one of the devices, Fig. 3 shows the $\Delta f/f_0$, and the TCD for the $\Psi=170^\circ$ mode. The agreement with measured and calculated values for both propagation properties can be seen throughout the entire temperature range. Also plotted for comparison in Fig. 3 are the $\Delta f/f_0$ and TCD predicted using the material constants and temperature coefficients from [2], the only reference publishing the entire set of constants needed to calculate these quantities, including the thermal coefficient of expansion, which as critical in the calculation as seen from (7).

D. Zero TCD Orientations

As can be seen from Fig. 2, the $\Psi=119^\circ$ and $\Psi=123^\circ$ SAWs lie in a region of space with very low or zero calculated TCD and electromechanical coupling nearly seven times that of ST-X quartz. Fig. 4 presents the measured and predicted temperature behavior along one of these orientations, namely $\Psi=123^\circ$. From Fig. 4a, it can be noted that the variation in frequency is less than 0.5 parts per thousand over the entire temperature range measured. The agreement between measured TCD (blue markers) and predicted TCD (red line) is

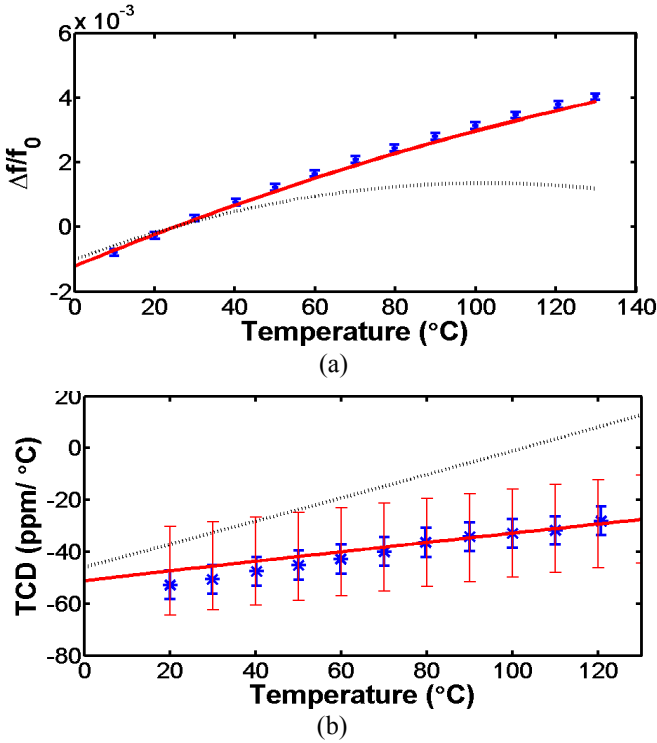


Figure 3. a) $\Delta f/f_0$ and b) TCD for the $\Psi=170^\circ$ SAW. Blue markers represent experimental points. Red and black traces are predicted values using constants in [9] and [2], respectively. Agreement between predicted temperature parameters and experiment are representative of all SAWs measured.

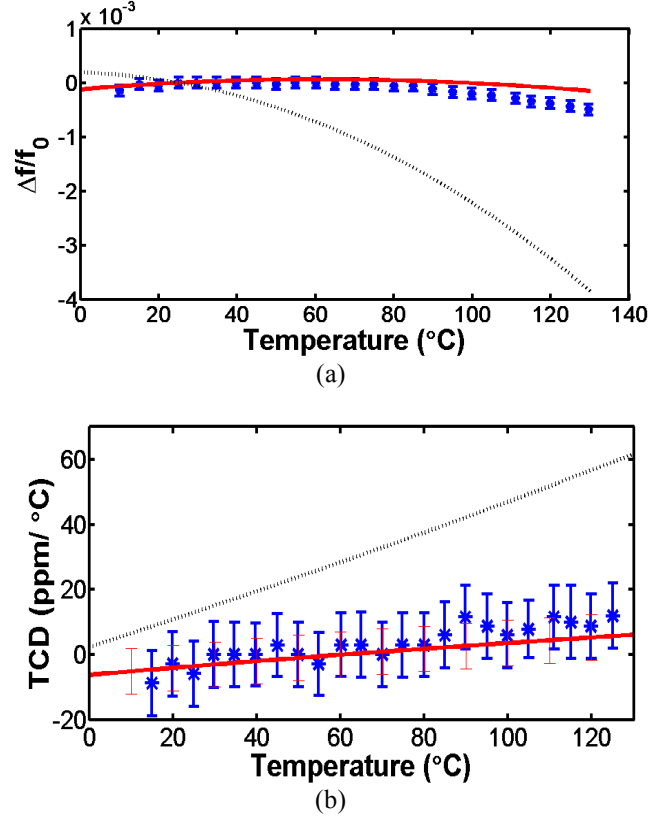


Figure 4. a) $\Delta f/f_0$ and b) TCD for the $\Psi=123^\circ$ SAW. This mode exhibits zero TCD in the vicinity of room temperature and a normalized frequency variation of less than five parts per thousand over a 120 °C temperature span. Blue markers represent experimental points. Red and black traces are predicted values using constants in [9] and [2], respectively.

excellent over the entire temperature range measured. A linear fit (not shown) to the measured *TCDs* for the $\Psi=123^\circ$ SAW yields a value of zero *TCD* at 50 °C. A similar case was found for the $\Psi=119^\circ$ mode, where the zero *TCD* identified by a linear fit to the data is at 60 °C. As suggested by Fig. 2 and supported by measurements of the $\Psi=119^\circ$, 123° modes (Fig. 4 and Table II), SAWs with Euler angles (90° , 23° , $110^\circ < \Psi < 130^\circ$) and in the neighborhood of space defined by ($90^\circ \pm \Delta$, $23^\circ \pm \Delta$, $110^\circ < \Psi < 130^\circ$) with Δ a variation around those angles, are very promising due to their low frequency variation with respect to temperature changes and their predicted coupling up to 0.75%.

V. CONCLUSIONS

The accuracy of a recently reported set of langatate material constants was investigated through the use of surface acoustic wave delay line measurements. The frequency response of devices aligned along seven orientations within the (90° , 23° , Ψ) plane were measured as a function of temperature. The room temperature phase velocities and the temperature coefficient of delay over a temperature range of 120 °C were found to be in agreement with predictions within the uncertainty limits of both the measurements and predictions.

A method for estimating the uncertainty in calculated SAW propagation properties such as phase velocity and temperature coefficient of delay based upon uncertainties in the fundamental material constants was developed and discussed.

A new LGT plane with an orientation region exhibiting both predicted coupling of $\sim 0.7\%$ and temperature compensation around room temperature was uncovered. The orientation (90° , 23° , 123°) in particular was verified to have less than 0.5 parts per thousand frequency variation over the entire temperature range measured (10 °C to 130 °C). The (90° , 23° , 119°) and (90° , 23° , 123°) orientations were found to have turnover temperatures at 60 and 50 °C, respectively.,

The SAW plane selected successfully validated the previously measured constants by the UMaine group for the temperature range between 10 °C to 130 °C.

ACKNOWLEDGMENT

The authors gratefully acknowledge Mr. Bennett Meulendyk and Mr. Peter Davulis of the Laboratory for Surface Science & Technology at UMaine for their assistance in the SAW device fabrication and in the hours spent on sample polishing.

REFERENCES

- [1] B. Chai, J. L. Lefaucheur, Y. Y. Ji, and H. Qiu, "Growth and evaluation of large size LGS ($\text{La}_3\text{Ga}_5\text{SiO}_{14}$), LGN ($\text{La}_3\text{Ga}_5\text{Nb}_{0.5}\text{O}_{14}$) & LGT ($\text{La}_3\text{Ga}_5\text{Ta}_{0.5}\text{O}_{14}$) single crystals," Proc. 1998 IEEE Int'l. Freq. Cont. Symp., pp 748-760.
- [2] M. Pereira da Cunha, D. C. Malocha, E. L. Adler, K. J. Casey, "Surface and pseudo surface acoustic waves in langatate: predictions and measurements," IEEE Trans. Ultrason., Ferroelect., Freq. Cont., vol 49, pp 1291-1299, September 2002.
- [3] Y. V. Pisarevsky, P.A. Senyushenkov, B.V. Mill, N.A. Moiseeva, "Elastic, piezoelectric, dielectric properties of $\text{La}_3\text{Ga}_5\text{Ta}_{0.5}\text{O}_{14}$ single crystals," Proc. 1998 IEEE Int'l. Freq. Cont. Symp., pp 742-747.
- [4] J. Bohm, E. Chilla, C. Flannery, H.J. Frohlich, T. Hauke, R.B. Heimann, M. Hengst, U. Straube, "Czochralski growth and characterization of piezoelectric single crystals with langasite structure: $\text{La}_3\text{Ga}_5\text{SiO}_{14}$ (LGS), $\text{La}_3\text{Ga}_5\text{Nb}_{0.5}\text{O}_{14}$ (LGN) and $\text{La}_3\text{Ga}_5\text{Ta}_{0.5}\text{O}_{14}$ (LGT) II. Piezoelectric and elastic properties," Journal of Crystal Growth, vol 216, pp 293-298, 2000.
- [5] N. Onozato, M. Adachi, T. Karaki, "Surface acoustic wave properties of $\text{La}_3\text{Ta}_{0.5}\text{Ga}_{5.5}\text{O}_{14}$ single crystals," Jpn. J. Appl. Phys., vol 39, pp 3028-3031, May 2000.
- [6] J. Schreuer, "Elastic and piezoelectric properties of $\text{La}_3\text{Ga}_5\text{SiO}_{14}$ and $\text{La}_3\text{Ga}_5\text{Ta}_{0.5}\text{O}_{14}$: an application of resonant ultrasound spectroscopy," IEEE Trans. Ultrason., Ferroelect., Freq. Cont., vol 49, pp 1474-1479, November 2002.
- [7] D. C. Malocha, M. Pereira da Cunha, E. Adler, R. C. Smythe, S. Frederick, M. Chou, R. Helmbold, Y. S. Zhou, "Recent measurements of material constants versus temperature for langatate, langanite, and langasite," Proc. 2000 IEEE Int'l Freq. Cont. Symp., pp 200-205.
- [8] E. Chilla, C. M. Flannery, and H. J. Frohlich, "Elastic properties of langasite-type crystals determined by bulk and surface acoustic waves," J. Appl. Phys., vol. 90, pp 6084-6091, December 2001.
- [9] B.T. Sturtevant, P.M. Davulis, and M. Pereira da Cunha, "Pulse echo and combined resonance techniques: a full set of LGT acoustic wave constants and temperature coefficients," IEEE Trans. Ultrason., Ferroelect., Freq. Cont., vol 56, pp 788-797, April 2009.
- [10] P. Krempf, G. Scleizer, and W. Wallnofer, "Gallium Phosphate, Ga_3PO_4 : A new piezoelectric crystal material for high-temperature sensorics," Sensors and Actuators A, vol. 61, pp 361-363, 1997.
- [11] John A. Kosinski, "New piezoelectric substrates for SAW devices," International Journal of High Speed Electronics and Systems, vol. 10, No. 4, pp 1017-1068, 2000.
- [12] Mauricio Pereira da Cunha and Saulo de Azevedo Fagundes, "Investigation of recent quartz-like materials for SAW applications," IEEE Trans. Ultrason., Ferroelect., Freq. Cont., vol 46, pp 1583-1590, November 1999.
- [13] J. Schreuer, C. Thybaut, M. Prestat, J. Stade, and E. Haussuhl, "Towards an understanding of the anomalous electromechanical behaviour of langasite and related compounds at high temperatures," Proc. 2003 IEEE Int'l Ultrason. Symp., pp 196-199.
- [14] R. Fachberger, E. Riha, E. Born, and P. Pongratz, "Homogeneity of langasite and langatate wafers for acoustic wave applications," Proc. 2003 IEEE Int'l Ultrason. Symp., pp 100-109.
- [15] T.R. Beaucege, E.P. Beenfeldt, S.A. Speakman, W.D. Porter, E.A. Payzant, M. Pereira da Cunha, "Comparison of high temperature crystal lattice and bulk thermal expansion measurements of LGT single crystal," Proc. 2006 IEEE Int'l Freq. Cont. Symp., pp 658-663.
- [16] P. M. Davulis, B. T. Sturtevant, S. I. Duy, M. Pereira da Cunha, "Revisiting LGT dielectric constants and temperature coefficients up to 120 deg. C," Proc. 2007 Int'l Ultrason. Symp., pp 1397-1400.
- [17] L.D. Doucette, M. Pereira da Cunha, R. J. Lad, "Precise orientation of single crystals by a simple X-ray diffraction rocking curve method," Rev. Sci. Instr., vol. 76, 036106, (4 pages), 2005.
- [18] B.T. Sturtevant, M. Pereira da Cunha, and R.J. Lad, "Determination of the absolute orientation of langatate crystals using X-ray diffraction," Proc. 2008 Int'l Ultrason. Symp., pp 741-744.
- [19] J.A. Cowperthwaite and M. Pereira da Cunha, "Optimal orientation function for SAW devices," Proc. 2003 IEEE Int'l Freq. Cont. Symp., pp.881-887.
- [20] David P. Morgan, *Surface-Wave Devices for Signal Processing*, Elsevier, New York, 1991.